



**Impact Response of an
Energy Absorbing
Earcup**

By

Dennis F. Shanahan

Biodynamics Research Division

and

Albert I. King

**Wayne State University
Detroit, Michigan 48202**

September 1983

Approved for public release, distribution unlimited.

**U.S. Army Aeromedical Research Laboratory
Fort Rucker, Alabama 36362-0577**

NOTICE

Qualified Requesters

Qualified requesters may obtain copies from the Defense Technical Information Center (DTIC), Cameron Station, Alexandria, Virginia. Orders will be expedited if placed through the librarian or other person designated to request documents from DTIC.

Change of Address

Organizations receiving reports from the US Army Aeromedical Research Laboratory on automatic mailing lists should confirm correct address when corresponding about laboratory reports.

Disposition

Destroy this report when it is no longer needed. Do not return it to the originator.

Disclaimer

The views, opinions, and/or findings contained in this report are those of the author(s) and should not be construed as an official Department of the Army position, policy, or decision, unless so designated by other official documentation. Citation of trade names in this report does not constitute an official Department of the Army endorsement or approval of the use of such commercial items.

Reviewed:



AARON W. SCHOPPER, Ph.D.
LTC, MSC
Director, Biodynamics Research
Division

Released for Publication:



J. D. LaMOTHE, Ph.D.
LTC, MS
Chairman, Scientific Review
Committee



DUDLEY R. PRICE
Colonel, MC, SFS
Commanding

REPORT DOCUMENTATION PAGE		READ INSTRUCTIONS BEFORE COMPLETING FORM
1. REPORT NUMBER USAARL Report No. 83-14	2. GOVT ACCESSION NO.	3. RECIPIENT'S CATALOG NUMBER
4. TITLE (and Subtitle) IMPACT RESPONSE OF AN ENERGY ABSORBING EARcup		5. TYPE OF REPORT & PERIOD COVERED
		6. PERFORMING ORG. REPORT NUMBER
7. AUTHOR(s) Dennis F. Shanahan and Albert I. King		8. CONTRACT OR GRANT NUMBER(s)
9. PERFORMING ORGANIZATION NAME AND ADDRESS SGRD-UAD-IE US Army Aeromedical Research Laboratory Fort Rucker, Alabama 36362		10. PROGRAM ELEMENT, PROJECT, TASK AREA & WORK UNIT NUMBERS 62777A, 3M161102BS10, AG, 281
11. CONTROLLING OFFICE NAME AND ADDRESS US Army Aeromedical Research Laboratory Fort Rucker, Alabama 36362		12. REPORT DATE August 1983
		13. NUMBER OF PAGES 40
14. MONITORING AGENCY NAME & ADDRESS (if different from Controlling Office)		15. SECURITY CLASS. (of this report) Unclassified
		15a. DECLASSIFICATION/DOWNGRADING SCHEDULE
16. DISTRIBUTION STATEMENT (of this Report) Approved for public release; distribution unlimited.		
17. DISTRIBUTION STATEMENT (of the abstract entered in Block 20, if different from Report)		
18. SUPPLEMENTARY NOTES This report was presented at the Tenth Annual International Workshop on Human Subjects for Biomechanical Research on 19 October 1982, Ann Arbor, Michigan		
19. KEY WORDS (Continue on reverse side if necessary and identify by block number) Flight helmet Aircraft accident Head injury Earcup		
20. ABSTRACT (Continue on reverse side if necessary and identify by block number) See back of form.		

Twelve impact tests on instrumented human cadavers were performed at Wayne State University to compare the load attenuating capability of an energy absorbing earcup with that of the standard rigid earcup used in SPH-4 flight helmets. SPH-4 helmeted cadavers were dropped from heights varying from 1.17 to 2.03 m. so as to receive a direct impact to the right side of the helmet. The helmet was equipped with either standard or energy absorbing earcups. Loads were measured at the impact surface and accelerations were measured through a triaxial accelerometer mounted to the cadaver's maxilla. Analysis of the data shows a significant decrease in both peak load and acceleration in the y axis for the energy absorbing earcup equipped helmets over those measured for the standard earcup equipped helmets.

TABLE OF CONTENTS

	PAGE NO.
List of Illustrations	4
List of Tables	4
Introduction	5
Materials and Methods	6
Results	7
Discussion	14
Conclusions	15
Bibliography	16
Appendixes	
Appendix A - Anthropometry of Test Subjects	17
Appendix B - Force and Acceleration Tracings from Test 001-015	31
Appendix C - List of Companies	40

LIST OF ILLUSTRATIONS

FIGURE		PAGE NO.
1	Photograph of Test Apparatus	6
2	Comparison of Force for EA and Standard Earcups	10
3	Comparison of Head Lateral (y-axis) Acceleration for EA and Standard Earcups	11
4	Comparison of Resultant Head Acceleration for EA and Standard Earcups	11
5	Impacted Helmet in Test 009	12
6	EA Earcups Used in Test 009	13
7	Standard Earcup from the Impacted Helmet Used in Test 013	13

LIST OF TABLES

TABLE		PAGE NO.
1	Summary of Anthropometric Data and Drop Heights	8
2	EA vs Standard Earcup - 2.03-m Drop Tests - Average Peak Values \pm 1 S. D.	9
3	EA vs Standard Earcup - 2.03-m Drop Tests - Results of Unpaired t-Tests	9
4	Measured Compression of Energy Absorbing Earcups	14

INTRODUCTION

For the past 12 years the U.S. Army Aeromedical Research Laboratory (USAARL) at Fort Rucker, AL, has been involved in a program of evaluating the impact performance of aviator flight helmets retrieved from aviation accidents. From these evaluations, it has become evident the current Army flight helmet, the Sound Protective Helmet Number Four (SPH-4) (Department of the Army, 1975), is relatively deficient in its ability to protect wearers against impacts to the lateral portions of the helmet (Haley and others, 1983; Shanahan, in press). It is believed this is due to there essentially being no energy absorbing material interposed between the helmet shell and the hard plastic circumaural housing for the communications headphones. There is a foam liner incorporated into the superior portions of the helmet, but it does not generally extend below the "hatband" region of the head at the sides of the helmet. Consequently, the force of an impact directed at the earcup region of the helmet is transmitted to the head of the wearer with relatively little attenuation other than that provided by the bending deformation effect of the helmet shell itself.

Accident statistics indicate that 26% of all impacts to the SPH-4 have occurred in the earcup region, and impacts in this area are known to result in substantially more severe injury than impacts to other areas of the helmet (Haley and others, 1983; Shanahan, in press). To provide increased impact protection to the earcup region of the helmet, a crushable energy-absorbing earcup was developed to be a direct replacement for the standard plastic earcup.

The modified earcup is constructed of 1 mm (0.040 inch) thick aluminum and is designed to provide 25 mm of crush at a maximum load of 4500 N. The crush distance was selected based on available space within the current helmet so modification of the helmet shell would not be required. The load limit of 4500 N arbitrarily was selected based on the little data available on human tolerance to impact in the temporoparietal area of the skull (Gurdjian, Lissner, Webster, 1974; Schneider, Naham, 1972; Travis, Stalnaker, Melvin, 1977). This load level is admittedly relatively high, being close to fracture threshold for localized impacts in the temporo-parietal area (Schneider, Naham, 1972; Travis, Stalnaker, Melvin, 1977). However, the size of the earcup allows loads to be spread over a large surface area (7900 mm²) and, because of the limited stroke distance available, a relatively high load limit had to be used.

Acoustical testing of the energy-absorbing earcup has shown it provides sound attenuating capability equivalent to the standard earcup. Initial impact tests were carried out utilizing a flat rigid mass dropped onto a helmet-earcup segment in a standard impact of 90 Nm (66 ft-lb) input energy (Haley and others, 1983). The energy-absorbing earcup transmitted a peak load of 4500 N whereas peak loads for the standard earcup were five times this level.

Clearly the new energy-absorbing earcup provides increased load attenuating capability over the current design. Nevertheless, since many assumptions were made in selecting the load limit for the earcup and since only isolated helmet segments had been impact tested, it was felt that helmeted cadaver impact tests would add useful information for validating the crushable earcup concept.

MATERIALS AND METHODS

The experimental design called for a whole-body drop test which would result in the impact of the helmeted head against a rigid surface. The rest of the body was to impact a cushioned surface so that the effect of body deceleration on head impact would be minimized. A drawing of the test apparatus is shown in Figure 1. The rigid impact surface consisted of a compression-type load cell 150 mm in diameter (Robert A. Denton, Inc.), supported by a rigid steel frame. A canvas sling was used to hoist the helmeted subject to the desired drop height and to maintain proper body orientation prior to the drop. The subject was oriented with its sagittal plane parallel to the horizontal and its head and neck projecting from the sling (Figure 1). The head was placed in proper orientation with duct tape attached between the helmet and the suspension sling frame. The load cell frame was positioned to insure contact of the earcup portion of the helmet with the center of the load cell. A 200 mm thick foam mattress supported by a wire mesh frame

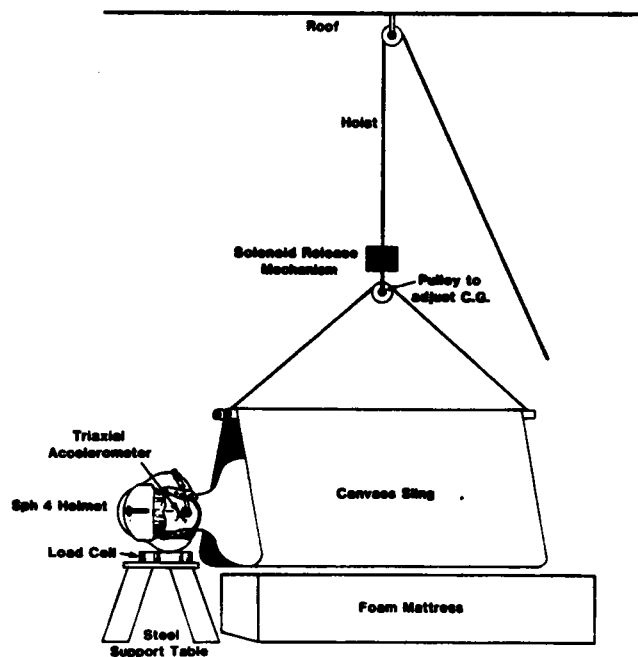


FIGURE 1. Photograph of Test Apparatus

was used to cushion the body upon impact. The height of the mattress was adjustable to permit the body to contact the mattress at or just before the time of head impact. The sling was suspended from a pulley system that allowed the drop height to be adjusted up to three meters. The test subject and sling were released by a solenoid-controlled release mechanism.

Cadavers used in these tests were obtained through the Wayne State University donor program and were instrumented with a triaxial accelerometer cluster of Endevco Model #2264 accelerometers. The accelerometer mount was firmly attached to the frontal aspect of the maxilla with bone screws. The sensitive axes of the accelerometer were oriented along the posterior-anterior (x) direction, the right-left (y) direction and the inferior-superior (z) direction. The impact was recorded on high speed film (400 fps) using a single camera placed in front of the impact assembly. Load cell and acceleration data were recorded on analog tape and filtered at 1000 Hz prior to digitization at 4000 Hz.

Embalmed cadavers were selected for these experiments based on age, anthropometry, and medical history. All subjects were younger than 69 (mean age of 60.2 with a range of 56-68), had no history of cancer or other prolonged debilitating diseases, and no previous history of skull or cervical fracture or surgery. Excessive obesity and craniometric measurements that did not correspond to available helmet sizes were reasons for rejection of a specimen. All potential test subjects underwent preimpact radiological examination of the head and neck. Evidence of preexisting fractures, marked structural abnormalities, or excessive osteoporosis were grounds for rejection of the cadaver. Anthropometric measurements of each of the 12 cadavers is presented in Appendix A.

Postimpact radiological examination of the head and neck was performed prior to autopsy. The skull was opened by removal of the calvarium, and the brain and dura excised to expose the inner surface of the skull to determine if any fractures had occurred. The skull then was separated from the neck at the atlanto-occipital junction and stripped of all coverings in order to examine the external surfaces for fracture.

The experimental apparatus was tested utilizing a DOT Part 572 50th percentile dummy prior to experimenting with cadavers. For these drops the method was identical to that described for the cadaver drops except that the triaxial accelerometer was mounted in the head of the dummy.

RESULTS

Twelve cadaver impacts were performed. Six cadavers were fitted with SPH-4 helmets equipped with standard earcups, and six were fitted with helmets equipped with energy-absorbing earcups. Additionally, three dummy impacts were performed for purposes of validating the test method. The drop height was varied from 1.17 m to 2.03 m. Table 1 is a summary of anthropometric data for the cadavers and the drop heights used for each of the 15

tests. There were no skull fractures in any cadaver drops. The only significant injury seen was a 45 mm curvilinear laceration in the scalp of the cadaver used in Test 005. The injury corresponded to the superior border of the standard plastic earcup used in that test. There were no lacerations on any of the cadavers fitted with energy-absorbing earcups.

Table 2 summarizes the average peak impact forces and average peak head x, y, and z accelerations measured for the standard and the energy-absorbing earcup tests performed at the 2.03 m drop-height. Table 3 shows the results of a t-test on unpaired samples performed on test data obtained from the seven cadaver tests at a drop-height of 2.03 m. It can be seen that the average load for the energy-absorbing earcup at 2.03 m was over 45% less than that measured for the standard earcup ($p < 0.05$). Likewise, the average head y-axis peak acceleration was 35% less ($p < 0.05$) for the energy-absorbing earcup drops. There was no significant difference for peak head accelerations in the x and z directions. Figures 2, 3, and 4 show a comparison

TABLE 1

SUMMARY OF ANTHROPOMETRIC DATA AND DROP HEIGHTS

TEST #	SUBJECT	AGE/ SEX	HEIGHT (m)	WEIGHT (kg)	HEAD CIRCUM. mm	%	DROP HT. (m)
001	DUMMY	-	-	76.0	584	87	1.17
002	DUMMY	-	-	76.0	584	87	1.17
003	CADAVER	58 F	1.630	84.0	603	>99	1.17
004	CADAVER	60 F	1.645	70.0	570	65	1.17
005	CADAVER	59 M	1.790	86.0	580	86	1.17
006	CADAVER	64 F	1.500	70.0	580	86	1.70
007	CADAVER	58 F	1.535	78.0	580	86	1.70
008	DUMMY	-	-	76.0	584	87	2.03
009	CADAVER	66 M	1.770	77.5	610	>99	2.03
010	CADAVER	66 F	1.555	75.3	610	>99	2.03
011	CADAVER	68 M	1.585	51.3	533	2	2.03
012	CADAVER	61 F	1.820	68.5	572	70	2.03
013	CADAVER	57 F	1.710	95.0	640	>99	2.03
014	CADAVER	56 F	*	56.0	585	92	2.03
015	CADAVER	59 F	1.585	79.0	610	>99	2.03

* Lower Extremities Double Amputee

of plots of load, head y-axis acceleration, and calculated resultant head acceleration for Tests 011 and 012. These data typify the differences seen between tests utilizing the two different earcup designs. A statistical analysis was not performed on the 1.17 m and 1.70 m drops. These drops were performed to test the experimental apparatus and to find a drop height that would provide approximately 50% crush of the energy-absorbing earcup. Load and acceleration tracings for these tests may be found in Appendix B.

TABLE 2

EA VS STANDARD EARCUP
2.03-m DROP TEST
AVERAGE PEAK VALUES \pm 1 S.D.

PARAMETER	IMPACT FORCE (N)		HEAD ACCELERATION (g)	
	y-AXIS	x-AXIS	y-AXIS	z-AXIS
EA EARCUP	5995 \pm 1256	37.0 \pm 8.2	121.0 \pm 22.7	50.3 \pm 17.2
STD. EARCUP	11039 \pm 2971	73.0 \pm 32.6	187.3 \pm 43.9	52.3 \pm 7.6

TABLE 3

EA VS STANDARD EARCUP
2.03-m DROP TEST
RESULTS OF UNPAIRED t-TESTS

PARAMETER	DF	t	p (%)
IMPACT FORCE	5	3.12	5 > p > 2.5
HEAD x-ACCELERATION	5	2.14	10 > p > 5.0
HEAD y-ACCELERATION	5	2.64	5 > p > 2.5
HEAD z-ACCELERATION	5	0.19	p > 50

Figure 5 is a photograph of the helmet impacted in Test 009. It is representative of the damage sustained by most of the helmets used in these tests. Note the scuffing and the horizontal fracture through the right earcup region of the helmet shell. Figure 6 shows the two energy-absorbing earcups used in this test. As expected, the left earcup was undamaged. The right earcup reveals the unsymmetrical nature of the loading it received during impact as most of the crushing is confined to the superior half of the earcup. The average compression was 6.9 mm or 27.6% of the available 25 mm. For purposes of comparison Figure 7 is a photograph of the standard earcup removed from the impacted side of the helmet used in Test 013. There is minimal damage to this earcup consisting only of a hairline fracture of the flange along the superior border of the earcup (see arrow). This was the maximum damage sustained by any of the standard earcups used in the cadaver impacts.

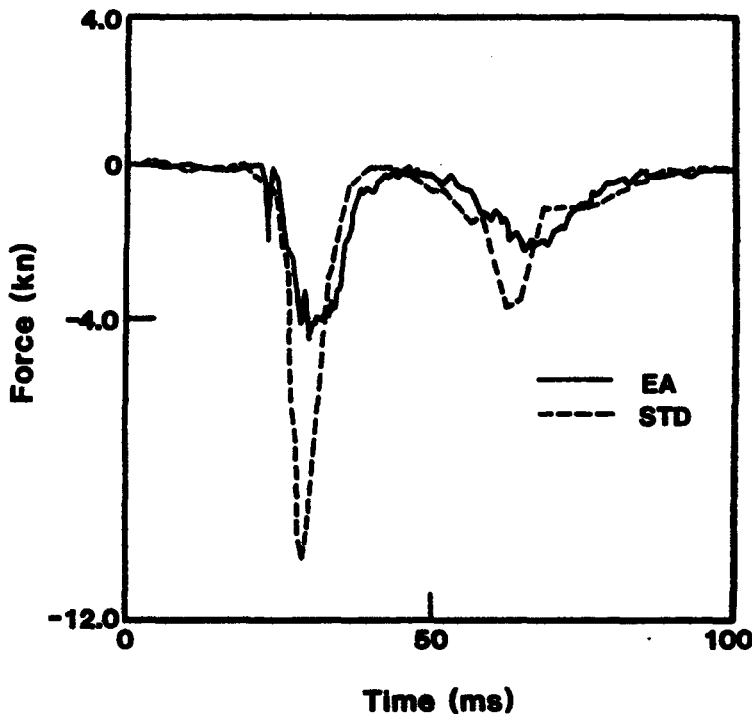


FIGURE 2. Comparison of Force for EA and Standard Earcups

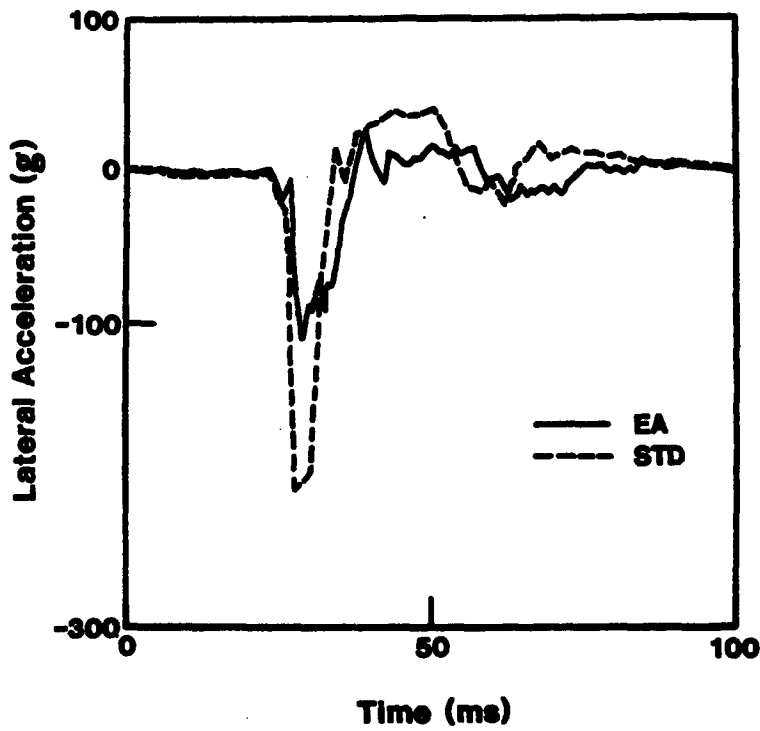


FIGURE 3. Comparison of Head Lateral (y-axis) Acceleration for EA and Standard Earcups

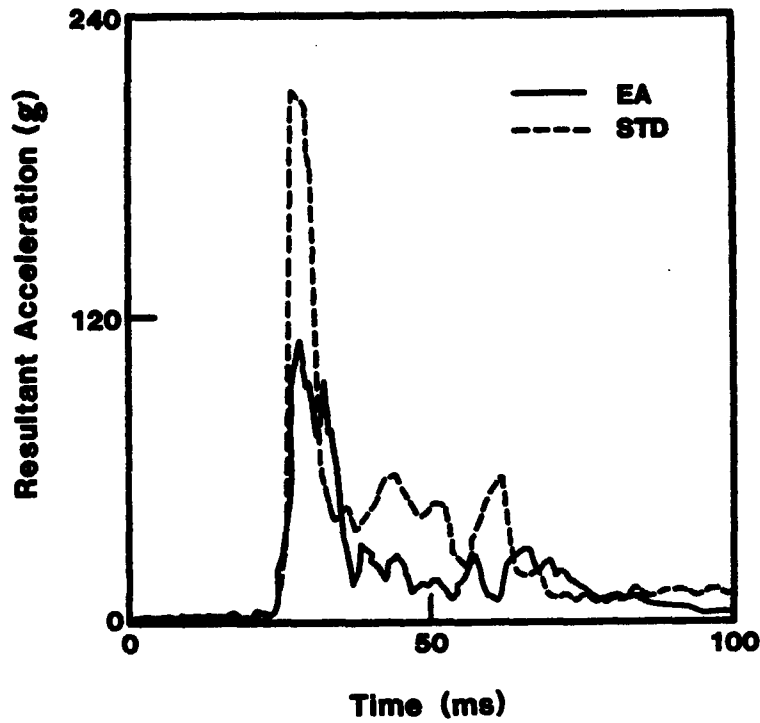


FIGURE 4. Comparison of Resultant Head Acceleration for EA and Standard Earcups

Table 4 is a summary of the measured compression for each of the energy-absorbing earcups used in this study. Since most of the earcups were not symmetrically loaded, a means of measuring average compression was developed. The point with the greatest compression and the point with the least compression were identified and a line drawn through them on the back of the earcup. A line perpendicular to this line passing through the center of the earcup then was drawn. Four measurements of height then were taken where the lines crossed the edges of the earcup. These heights were averaged and compared to the height of an undamaged earcup. This was the average loss in height or average permanent crush. This was compared to the total compression available (25 mm) and reported in Table 4 as a percentage of crush available. Note that the greatest permanent compression seen was 53%. However, based on the elasticity of aluminum, it is probable that the maximum dynamic compression depth was 8-12 percent greater, or 61-66%.

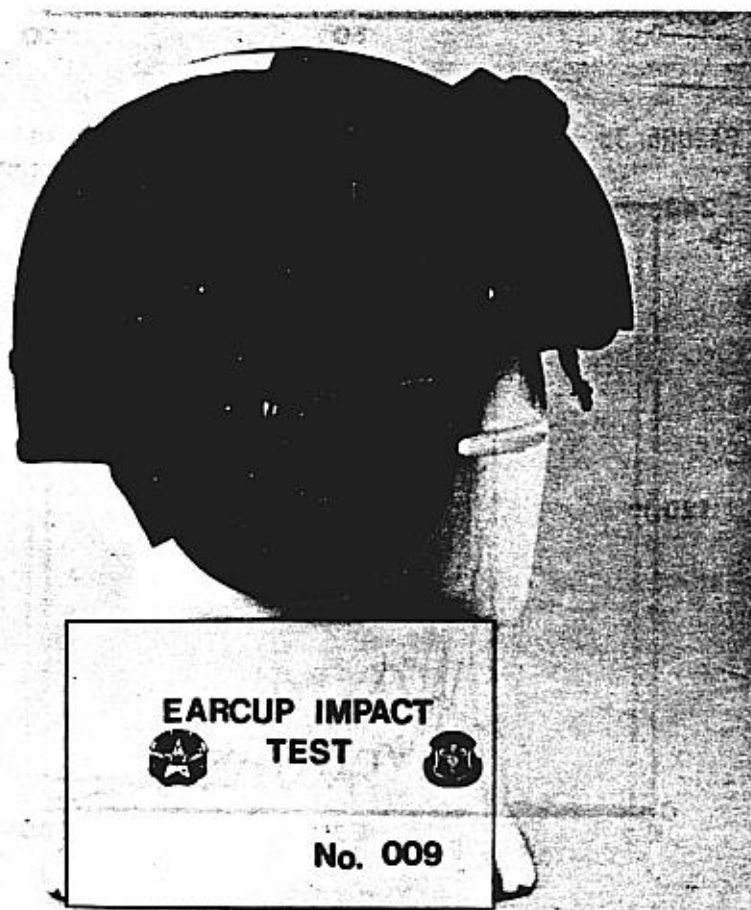


FIGURE 5. Impacted Helmet in Test 009

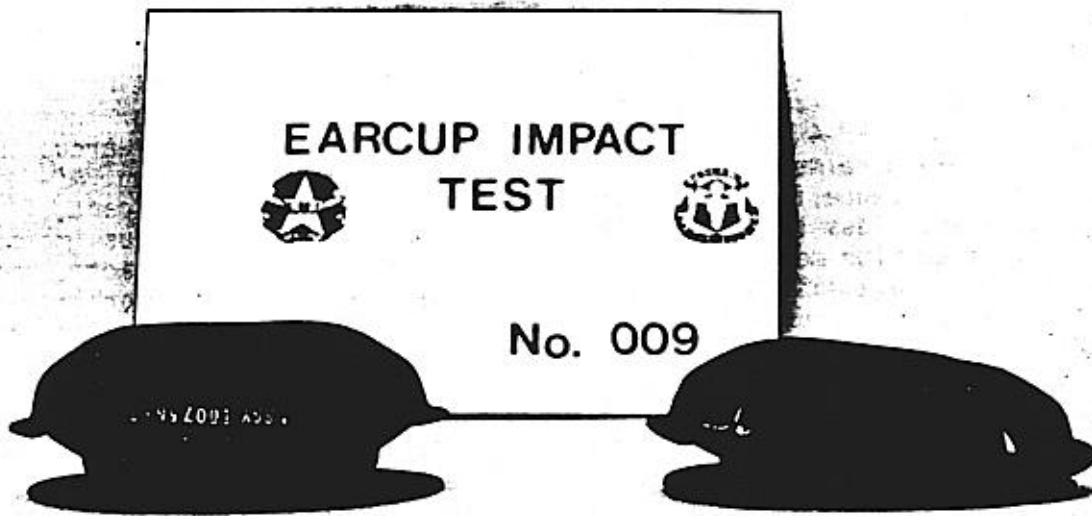


FIGURE 6. EA Earcups Used in Test 009

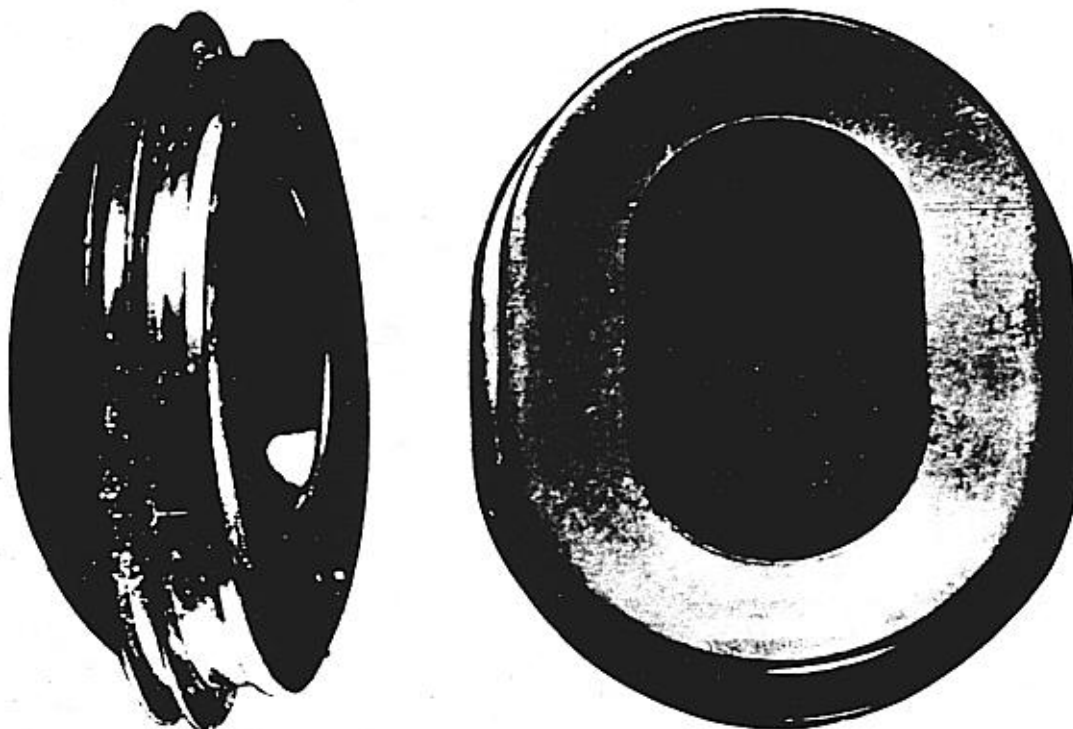


FIGURE 7. Standard Earcup from the Impacted Helmet Used in Test 013

DISCUSSION

In this series of blunt impacts to the earcup region of the helmet shell, peak loads and peak y-axis accelerations were considerably less for those subjects wearing SPH-4 helmets equipped with the energy-absorbing earcup than for those wearing helmets equipped with the standard plastic earcup. Although the difference in loads between the two earcups was significant, it was considerably less than expected based on the results of previous impact tests performed with metal headforms. In the helmeted cadaver impacts, there was only an average 45% reduction in peak loads for the energy-absorbing earcup for the 2.03 m drops as compared to loads measured for the standard earcup while the flat metal mass tests showed a 5-fold reduction at roughly equivalent input energies (Haley and others, 1983). There are several reasons for these discrepant results. In the flat metal mass tests, a metal mass was dropped vertically onto the earcup section of helmet shell with the earcup resting directly on the load cell. The entire load was transmitted directly through the shell to the earcup and the system was not free to rotate or translate.

In the helmeted cadaver impacts, the impact force was transmitted to the head not only through the earcup, but also through several points in the helmet shell and through the foam liner over the superior portion of the impacted side. These factors tended to reduce the loads delivered to the earcups

TABLE 4

MEASURED COMPRESSION OF ENERGY ABSORBING EARCUPS

TEST NO.	SUBJECT	DROP HEIGHT (m)	AVERAGE DEFORMATION (mm)	PERCENT OF AVAILABLE CRUSH
001	DUMMY	1.17	3.6	14
003	CADAVER	1.17	3.3	13
004	CADAVER	1.17	6.6	26
008	DUMMY	2.03	11.4	46
009	CADAVER	2.03	6.9	28
010	CADAVER	2.03	9.4	38
011	CADAVER	2.03	12.7	51
015	CADAVER	2.03	13.2	53

during the cadaver impacts. This situation reduced the difference in measured performance between the two earcup designs when compared to the metal headform drops since the condition aids the performance of the standard earcup and prevents the energy-absorbing earcup from realizing its full crush capacity for the input energy used in these tests.

At higher input energies, the difference in loads would be expected to become greater as the crushable earcup continued to limit the loads to the same approximate level seen in these experiments until it reached full crush. On the other hand, the rigid earcup would transmit increasingly higher loads as the input energy increased. This difference in measured loads between the two earcup designs in helmeted cadaver impacts would probably never attain the magnitude seen in the rather idealized metal mass tests for the reasons enumerated.

One major problem encountered in this study relates to the use of embalmed cadavers. Embalmed specimens were used since they were available much more readily than fresh cadavers. However, after embalming, the subcutaneous tissue in the scalp becomes engorged with embalming fluid and swells considerably. Whereas the thickness of the skin in the posterior auricular area in the live subject is normally only 2-3 mm, many of the cadavers used in this study had thicknesses approaching 15 mm. This situation is reflected by the preponderance of extremely large head circumferences seen in the cadavers used in this study (Table 1). Clearly, this artifactually-increased subcutaneous tissue depth provides the embalmed cadaver with a very high degree of impact attenuation capability not present in a live subject. This explains in large part why the relatively high input energies used in these experiments (approximately 136 Nm or 100 ft-lb for the 2.03-m drops) failed to produce skull fracture in the standard earcup tests or to produce high levels of crush in the energy-absorbing earcup tests (Table 4). In all probability, if fresh cadavers had been used, the same drop heights would have produced markedly greater loads and accelerations for the standard earcup tests and higher levels of crushing in the energy-absorbing earcups.

CONCLUSIONS

This study failed to provide any definitive data on the adequacy of the stroke level or distance selected for the energy-absorbing earcup. The engorged subcutaneous tissue in the scalp of the cadavers used appears to be the primary reason. There is no question that the energy-absorbing earcup offers significantly increased impact protection over the standard (rigid) earcup design, and this fact alone is believed sufficient to recommend its incorporation into all U.S. Army flight helmets. In the meantime, it is hoped that these experiments can be repeated, using fresh cadavers and perhaps a modified procedure to try to obtain more definitive data on the performance of the crushable earcup.

BIBLIOGRAPHY

- Churchill, E., McConville, J. T., Laubach, L. L., White, R. M. 1970. *Anthropometry of U.S. Army aviators - 1970*. Natick, MA: United States Army Natick Laboratories. TR-72-52-CE.
- Department of the Army. 1975. *Helmet, flyer's protection, SPH-4*, Natick, MA: United States Army Natick Research and Development Command. Mil-H-43925.
- Gurdjian, E. S., Lissner, H. R. and Webster, J. E. 1974. The mechanism of production of linear skull fracture. *Surgery, gynecology, and obstetrics*. 85:195-210.
- Haley, J. L., Shanahan, D. F., Reading, T. E. and Knapp, S. C. 1983. Head impact hazards in helicopter operations and their mitigation through improved helmet design. In: Ewing, C. L. (and others) (Eds.) *Impact injury of the head and spine*. C. C. Thomas, Springfield, IL.
- Schneider, D. C. and Naham, A. M. 1972. Impact studies of facial bones and skull. In: *Proceedings of the Sixteenth Stapp Car Crash Conference*. Society of Automotive Engineers, Inc. New York, NY.
- Shanahan, D. F. In press. Basilar skull fracture in U.S. Army aircraft accidents. *Aviation, space, and environmental medicine*.
- Travis, L. W., Stalnaker, R. L. and Melvin, J. W. 1977. Impact trauma of the human temporal bone. *The journal of trauma*. 17(10):761-766.

APPENDIX A
ANTHROPOMETRY OF TEST SUBJECTS

Subject Cadaver 5146, Female, Test 003Date 7-13-81Age - 58 yrs.

Measurement	Description	Millimeters
Standing Height	Heels, Shoulders, Buttocks & Head Erect	1630
Sitting Height	Head to Seat with Body Erect	895
Neck Breadth (y)	Lateral	105
Neck Depth (x)	A to P	125
Upper Torso Breadth (y)	Chest Breadth at Xiphoid	315
Shoulder Width (y)	Biachromial Breadth	350
Lower Torso Breadth (y)	Right to Left Iliocristale	390
Upper Leg Length (z)	Trochanter to Femoral Condyle	310
Lower Leg Length (z)	Tibiale to Heels	365
Head Height (z)	Gnathion to Vertex	230
Head Breadth (y)	Right to Left Tragion	150
Head Depth (x)	Ophistocranon to Glabella	185
Head Circumference	Above Brow Ridge	603
Upper Torso Depth (x)	Chest Depth at Xiphoid	225
Lower Torso Depth (x)	At Anterior-Superior Iliac Spine	225
Chest Circumference	At Xiphoid	940
Waist Circumference	At Most Superior Point of Pelvis	1070
Top of Head to C7		225
Neck Height (z)	C1 to C7	60
Upper Torso Height (z)	C7 to T12	335
T1 to T3 (z)	At Posterior Processes	40
T7 to T9 (z)	At Posterior Processes	40
L1 to L3 (z)	At Posterior Processes	40
Lower Torso Height (z)	T12 to Coccyx	275
Weight	Of Whole Body	84.0 kg

Subject Cadaver 5145, Female, Test 004

Date 7-13-81

Age - 60 yrs.

Measurement	Description	Millimeters
Standing Height	Heels, Shoulders, Buttocks & Head Erect	1645
Sitting Height	Head to Seat with Body Erect	830
Neck Breadth (y)	Lateral	110
Neck Depth (x)	A to P	110
Upper Torso Breadth (y)	Chest Breadth at Xiphoid	310
Shoulder Width (y)	Biachromial Breadth	350
Lower Torso Breadth (y)	Right to Left Iliocristale	380
Upper Leg Length (z)	Trochanter to Femoral Condyle	335
Lower Leg Length (z)	Tibiale to Heels	390
Head Height (z)	Gnathion to Vertex	225
Head Breadth (y)	Right to Left Tragion	160
Head Depth (x)	Ophistocranon to Glabella	175
Head Circumference	Above Brow Ridge	570
Upper Torso Depth (x)	Chest Depth at Xiphoid	210
Lower Torso Depth (x)	At Anterior-Superior Iliac Spine	210
Chest Circumference	At Xiphoid	900
Waist Circumference	At Most Superior Point of Pelvis	1015
Top of Head to C7		215
Neck Height (z)	C1 to C7	80
Upper Torso Height (z)	C7 to T12	290
T1 to T3 (z)	At Posterior Processes	50
T7 to T9 (z)	At Posterior Processes	40
L1 to L3 (z)	At Posterior Processes	55
Lower Torso Height (z)	T12 to Coccyx	240
Weight	Of Whole Body	70.0 kg

Subject Cadaver 5066, Male, Test 005Date 7-13-82

Age - 59 yrs.

Measurement		Description	Millimeters
Standing Height		Heels, Shoulders, Buttocks & Head Erect	1790
Sitting Height		Head to Seat with Body Erect	950
Neck Breadth	(y)	Lateral	120
Neck Depth	(x)	A to P	120
Upper Torso Breadth	(y)	Chest Breadth at Xiphoid	350
Shoulder Width	(y)	Biachromial Breadth	375
Lower Torso Breadth	(y)	Right to Left Iliocristale	360
Upper Leg Length	(z)	Trochanter to Femoral Condyle	340
Lower Leg Length	(z)	Tibiale to Heels	440
Head Height	(z)	Gnathion to Vertex	230
Head Breadth	(y)	Right to Left Tragion	155
Head Depth	(x)	Ophistocranon to Glabella	200
Head Circumference		Above Brow Ridge	580
Upper Torso Depth	(x)	Chest Depth at Xiphoid	240
Lower Torso Depth	(x)	At Anterior-Superior Iliac Spine	225
Chest Circumference		At Xiphoid	990
Waist Circumference		At Most Superior Point of Pelvis	990
Top of Head to C7			230
Neck Height	(z)	C1 to C7	70
Upper Torso Height	(z)	C7 to T12	335
T1 to T3	(z)	At Posterior Processes	65
T7 to T9	(z)	At Posterior Processes	70
L1 to L3	(z)	At Posterior Processes	55
Lower Torso Height	(z)	T12 to Coccyx	425
Weight		Of Whole Body	86.0 kg

Subject Cadaver 5161, Female, Test 006Date 7-27-81

Age - 64 yrs.

Measurement	Description	Millimeters
Standing Height	Heels, Shoulders, Buttocks & Head Erect	1500
Sitting Height	Head to Seat with Body Erect	805
Neck Breadth (y)	Lateral	110
Neck Depth (x)	A to P	125
Upper Torso Breadth (y)	Chest Breadth at Xiphoid	305
Shoulder Width (y)	Biachromial Breadth	320
Lower Torso Breadth (y)	Right to Left Iliocristale	315
Upper Leg Length (z)	Trochanter to Femoral Condyle	310
Lower Leg Length (z)	Tibiale to Heels	320
Head Height (z)	Gnathion to Vertex	220
Head Breadth (y)	Right to Left Tragion	155
Head Depth (x)	Ophistocranon to Glabella	175
Head Circumference	Above Brow Ridge	580
Upper Torso Depth (x)	Chest Depth at Xiphoid	245
Lower Torso Depth (x)	At Anterior-Superior Iliac Spine	235
Chest Circumference	At Xiphoid	910
Waist Circumference	At Most Superior Point of Pelvis	910
Top of Head to C7		200
Neck Height (z)	C1 to C7	45
Upper Torso Height (z)	C7 to T12	325
T1 to T3 (z)	At Posterior Processes	60
T7 to T9 (z)	At Posterior Processes	65
L1 to L3 (z)	At Posterior Processes	70
Lower Torso Height (z)	T12 to Coccyx	210
Weight	Of Whole Body	70.0 kg

Subject Cadaver 5155, Female, Test 007
Age - 58 yrs.

Date 7-28-81

Measurement	Description	Millimeters
Standing Height	Heels, Shoulders, Buttocks & Head Erect	1535
Sitting Height	Head to Seat with Body Erect	800
Neck Breadth (y)	Lateral	95
Neck Depth (x)	A to P	120
Upper Torso Breadth (y)	Chest Breadth at Xiphoid	310
Shoulder Width (y)	Biachromial Breadth	320
Lower Torso Breadth (y)	Right to Left Iliocristale	360
Upper Leg Length (z)	Trochanter to Femoral Condyle	325
Lower Leg Length (z)	Tibiale to Heels	410
Head Height (z)	Gnathion to Vertex	245
Head Breadth (y)	Right to Left Tragion	145
Head Depth (x)	Ophistocranon to Glabella	170
Head Circumference	Above Brow Ridge	580
Upper Torso Depth (x)	Chest Depth at Xiphoid	210
Lower Torso Depth (x)	At Anterior-Superior Iliac Spine	250
Chest Circumference	At Xiphoid	980
Waist Circumference	At Most Superior Point of Pelvis	980
Top of Head to C7		200
Neck Height (z)	C1 to C7	35
Upper Torso Height (z)	C7 to T12	310
T1 to T3 (z)	At Posterior Processes	40
T7 to T9 (z)	At Posterior Processes	40
L1 to L3 (z)	At Posterior Processes	50
Lower Torso Height (z)	T12 to Coccyx	195
Weight	Of Whole Body	78.0 kg

Subject Cadaver 5236, Male, Test 009
 Age - 56 yrs.

Date 12-14-81

Measurement	Description	Millimeters
Standing Height	Heels, Shoulders, Buttocks & Head Erect	1770
Sitting Height	Head to Seat with Body Erect	840
Neck Breadth (y)	Lateral	125
Neck Depth (x)	A to P	125
Upper Torso Breadth (y)	Chest Breadth at Xiphoid	340
Shoulder Width (y)	Biachromial Breadth	380
Lower Torso Breadth (y)	Right to Left Iliocristale	350
Upper Leg Length (z)	Trochanter to Femoral Condyle	425
Lower Leg Length (z)	Tibiale to Heels	485
Head Height (z)	Gnathion to Vertex	235
Head Breadth (y)	Right to Left Tragion	170
Head Depth (x)	Ophistocranon to Glabella	205
Head Circumference	Above Brow Ridge	620
Upper Torso Depth (x)	Chest Depth at Xiphoid	250
Lower Torso Depth (x)	At Anterior-Superior Iliac Spine	220
Chest Circumference	At Xiphoid	1028
Waist Circumference	At Most Superior Point of Pelvis	953
Top of Head to C7		205
Neck Height (z)	C1 to C7	195
Upper Torso Height (z)	C7 to T12	355
T1 to T3 (z)	At Posterior Processes	55
T7 to T9 (z)	At Posterior Processes	75
L1 to L3 (z)	At Posterior Processes	55
Lower Torso Height (z)	T12 to Coccyx	235
Weight	Of Whole Body	77.5 kg

Subject Cadaver 5211, Female, Test 010
 Age - 66 yrs.

Date 12-15-81

Measurement		Description	Millimeters
Standing Height		Heels, Shoulders, Buttocks & Head Erect	1555
Sitting Height		Head to Seat with Body Erect	880
Neck Breadth	(y)	Lateral	130
Neck Depth	(x)	A to P	130
Upper Torso Breadth	(y)	Chest Breadth at Xiphoid	315
Shoulder Width	(y)	Biachromial Breadth	360
Lower Torso Breadth	(y)	Right to Left Iliocristale	325
Upper Leg Length	(z)	Trochanter to Femoral Condyle	350
Lower Leg Length	(z)	Tibiale to Heels	425
Head Height	(z)	Gnathion to Vertex	230
Head Breadth	(y)	Right to Left Tragion	155
Head Depth	(x)	Ophistocranon to Glabella	180
Head Circumference		Above Brow Ridge	610
Upper Torso Depth	(x)	Chest Depth at Xiphoid	235
Lower Torso Depth	(x)	At Anterior-Superior Iliac Spine	285
Chest Circumference		At Xiphoid	940
Waist Circumference		At Most Superior Point of Pelvis	965
Top of Head to C7			220
Neck Height	(z)	C1 to C7	40
Upper Torso Height	(z)	C7 to T12	330
T1 to T3	(z)	At Posterior Processes	60
T7 to T9	(z)	At Posterior Processes	75
L1 to L3	(z)	At Posterior Processes	75
Lower Torso Height	(z)	T12 to Coccyx	220
Weight		Of Whole Body	75.0 kg

Subject Cadaver 5246, Male, Test 011
 Age - 68 yrs.

Date 12-15-81

Measurement	Description	Millimeters
Standing Height	Heels, Shoulders, Buttocks & Head Erect	1585
Sitting Height	Head to Seat with Body Erect	850
Neck Breadth (y)	Lateral	105
Neck Depth (x)	A to P	95
Upper Torso Breadth (y)	Chest Breadth at Xiphoid	270
Shoulder Width (y)	Biachromial Breadth	305
Lower Torso Breadth (y)	Right to Left Iliocristale	280
Upper Leg Length (z)	Trochanter to Femoral Condyle	380
Lower Leg Length (z)	Tibiale to Heels	405
Head Height (z)	Gnathion to Vertex	205
Head Breadth (y)	Right to Left Tragion	140
Head Depth (x)	Ophistocranon to Glabella	150
Head Circumference	Above Brow Ridge	533
Upper Torso Depth (x)	Chest Depth at Xiphoid	185
Lower Torso Depth (x)	At Anterior-Superior Iliac Spine	150
Chest Circumference	At Xiphoid	813
Waist Circumference	At Most Superior Point of Pelvis	737
Top of Head to C7		200
Neck Height (z)	C1 to C7	70
Upper Torso Height (z)	C7 to T12	305
T1 to T3 (z)	At Posterior Processes	50
T7 to T9 (z)	At Posterior Processes	60
L1 to L3 (z)	At Posterior Processes	50
Lower Torso Height (z)	T12 to Coccyx	225
Weight	Of Whole Body	51.2 kg

Subject Cadaver 5213, Female, Test 012
Age - 61 yrs.

Date 12-15-81

Measurement	Description	Millimeters
Standing Height	Heels, Shoulders, Buttocks & Head Erect	1820
Sitting Height	Head to Seat with Body Erect	895
Neck Breadth (y)	Lateral	110
Neck Depth (x)	A to P	90
Upper Torso Breadth (y)	Chest Breadth at Xiphoid	345
Shoulder Width (y)	Biachromial Breadth	305
Lower Torso Breadth (y)	Right to Left Iliocristale	380
Upper Leg Length (z)	Trochanter to Femoral Condyle	380
Lower Leg Length (z)	Tibiale to Heels	425
Head Height (z)	Gnathion to Vertex	225
Head Breadth (y)	Right to Left Tragion	140
Head Depth (x)	Ophistocranon to Glabella	170
Head Circumference	Above Brow Ridge	572
Upper Torso Depth (x)	Chest Depth at Xiphoid	215
Lower Torso Depth (x)	At Anterior-Superior Iliac Spine	210
Chest Circumference	At Xiphoid	1029
Waist Circumference	At Most Superior Point of Pelvis	1029
Top of Head to C7		240
Neck Height (z)	C1 to C7	50
Upper Torso Height (z)	C7 to T12	330
T1 to T3 (z)	At Posterior Processes	65
T7 to T9 (z)	At Posterior-Processes	65
L1 to L3 (z)	At Posterior Processes	65
Lower Torso Height (z)	T12 to Coccyx	100
Weight	Of Whole Body	68.5 kg

Age - 57 yrs.

Measurement		Description	Millimeters
Standing Height		Heels, Shoulders, Buttocks & Head Erect	1710
Sitting Height		Head to Seat with Body Erect	920
Neck Breadth	(y)	Lateral	130
Neck Depth	(x)	A to P	170
Upper Torso Breadth	(y)	Chest Breadth at Xiphoid	350
Shoulder Width	(y)	Biachromial Breadth	380
Lower Torso Breadth	(y)	Right to Left Iliocristale	345
Upper Leg Length	(z)	Trochanter to Femoral Condyle	460
Lower Leg Length	(z)	Tibiale to Heels	420
Head Height	(z)	Gnathion to Vertex	265
Head Breadth	(y)	Right to Left Tragion	170
Head Depth	(x)	Ophistocranon to Glabella	205
Head Circumference		Above Brow Ridge	640
Upper Torso Depth	(x)	Chest Depth at Xiphoid	250
Lower Torso Depth	(x)	At Anterior-Superior Iliac Spine	270
Chest Circumference		At Xiphoid	990
Waist Circumference		At Most Superior Point of Pelvis	1040
Top of Head to C7			280
Neck Height	(z)	C1 to C7	115
Upper Torso Height	(z)	C7 to T12	320
T1 to T3	(z)	At Posterior Processes	60
T7 to T9	(z)	At Posterior Processes	55
L1 to L3	(z)	At Posterior Processes	75
Lower Torso Height	(z)	T12 to Coccyx	250
Weight		Of Whole Body	95.0 kg

Age - 56 yrs.

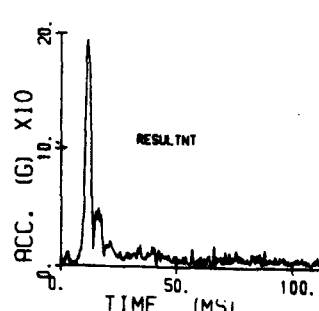
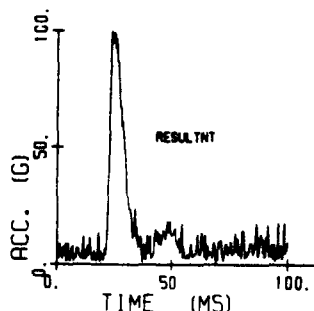
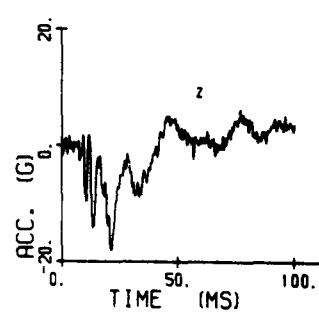
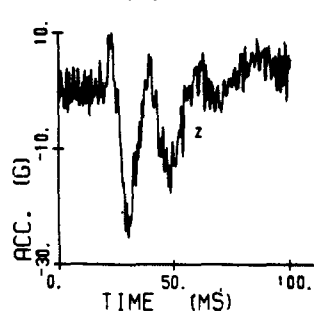
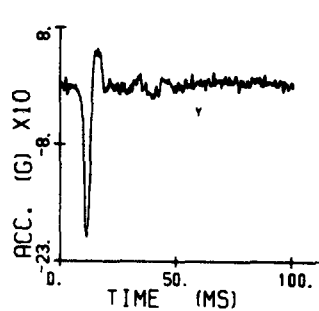
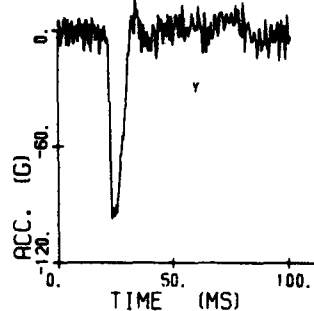
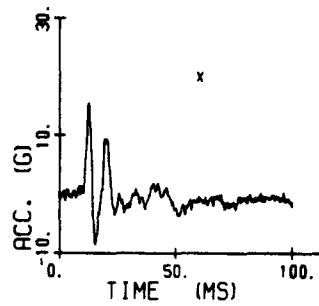
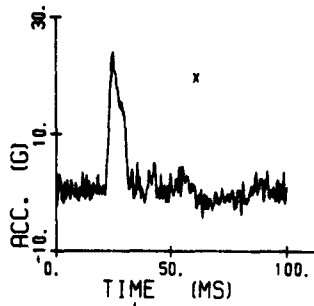
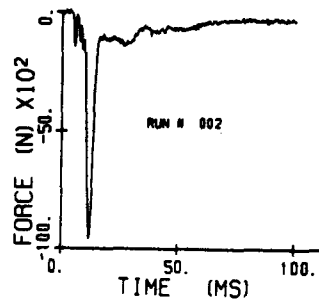
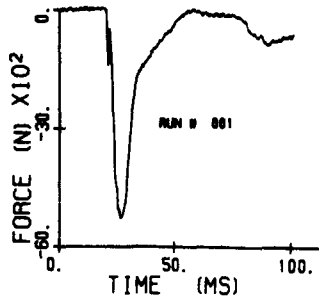
Measurement	Description	Millimeters
Standing Height	Heels, Shoulders, Buttocks & Head Erect	*
Sitting Height	Head to Seat with Body Erect	870
Neck Breadth (y)	Lateral	130
Neck Depth (x)	A to P	120
Upper Torso Breadth (y)	Chest Breadth at Xiphoid	350
Shoulder Width (y)	Biachromial Breadth	390
Lower Torso Breadth (y)	Right to Left Iliocristale	355
Upper Leg Length (z)	Trochanter to Femoral Condyle	360
Lower Leg Length (z)	Tibiale to Heels	*
Head Height (z)	Gnathion to Vertex	270
Head Breadth (y)	Right to Left Tragion	160
Head Depth (x)	Ophistocranon to Glabella	195
Head Circumference	Above Brow Ridge	585
Upper Torso Depth (x)	Chest Depth at Xiphoid	240
Lower Torso Depth (x)	At Anterior-Superior Iliac Spine	255
Chest Circumference	At Xiphoid	1015
Waist Circumference	At Most Superior Point of Pelvis	1070
Top of Head to C7		245
Neck Height (z)	C1 to C7	80
Upper Torso Height (z)	C7 to T12	320
T1 to T3 (z)	At Posterior Processes	60
T7 to T9 (z)	At Posterior Processes	50
L1 to L3 (z)	At Posterior Processes	35
Lower Torso Height (z)	T12 to Coccyx	215
Weight	Of Whole Body	75.0 kg

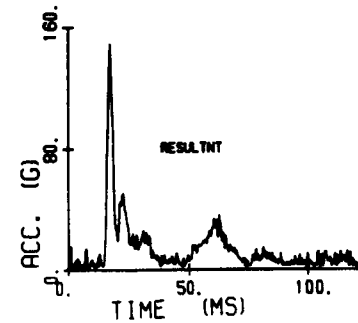
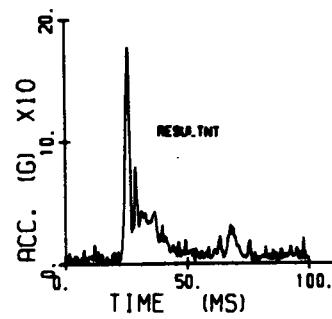
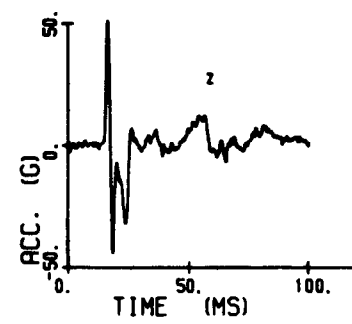
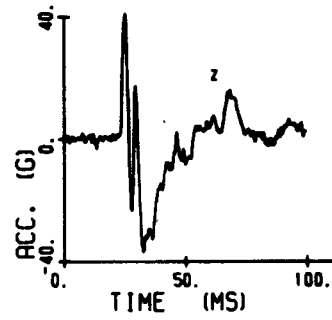
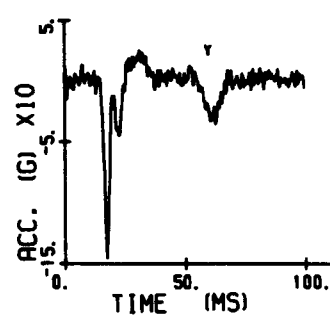
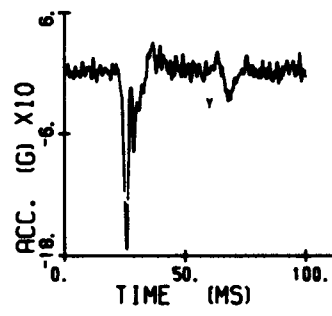
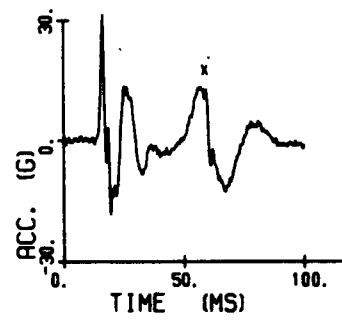
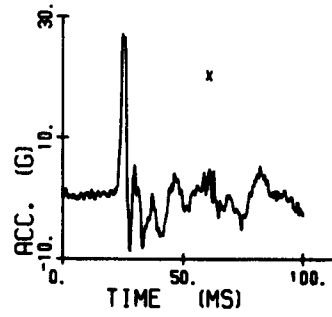
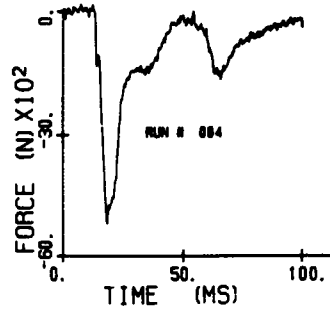
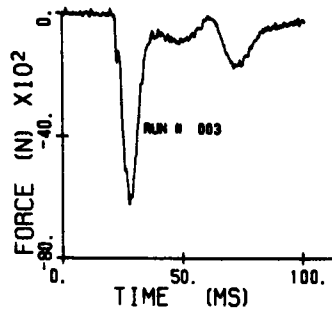
* Specimen had bilateral below-knee amputations.

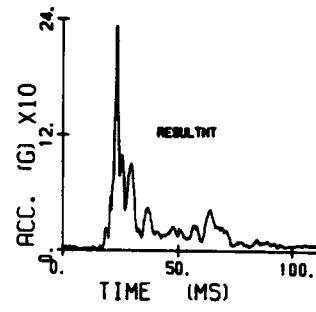
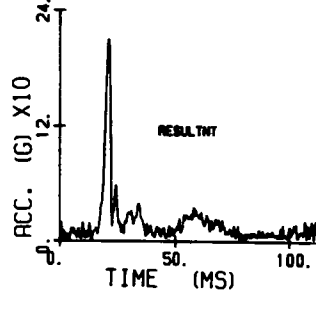
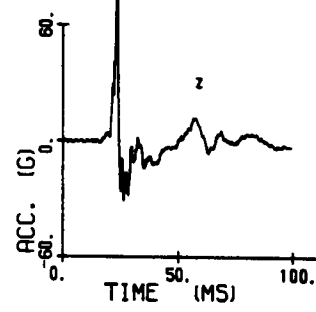
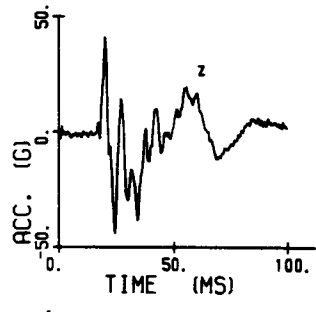
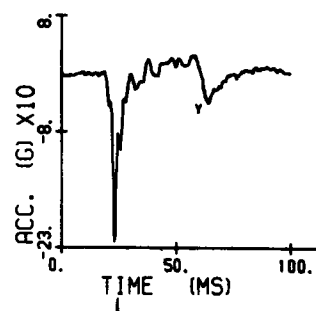
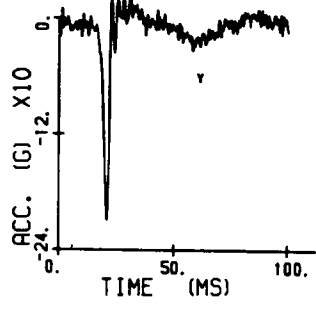
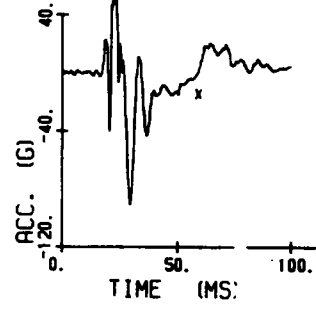
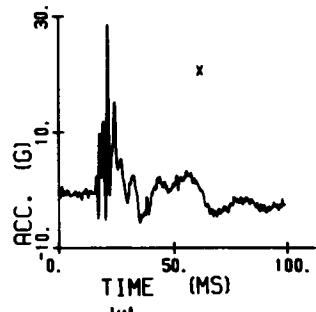
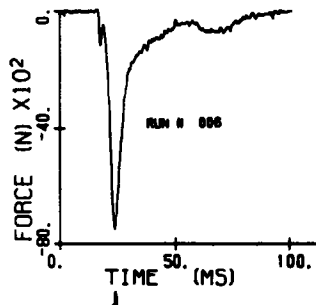
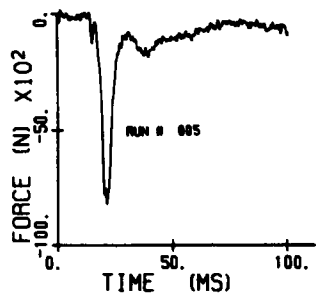
Age - 59 yrs.

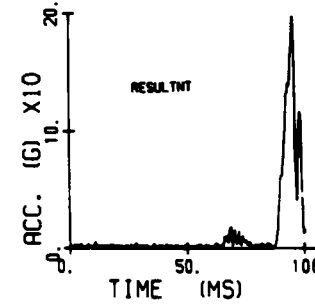
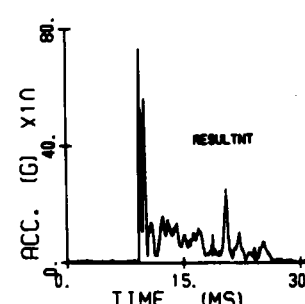
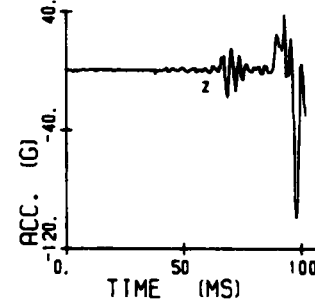
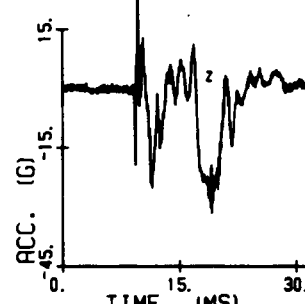
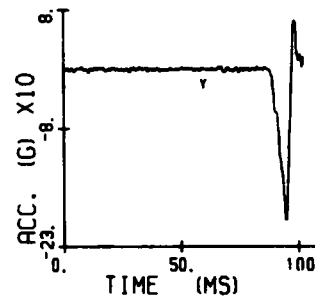
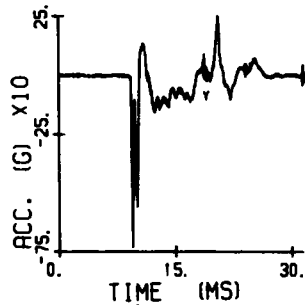
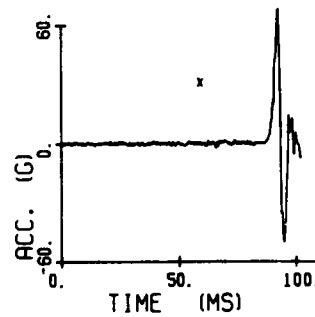
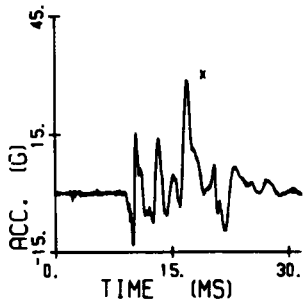
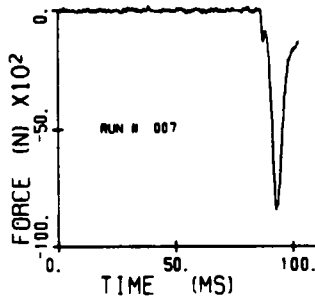
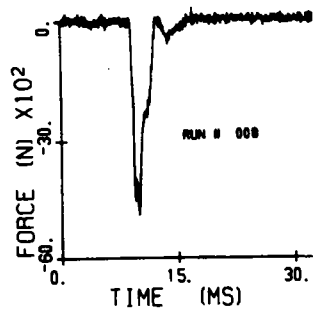
Measurement		Description	Millimeters
Standing Height		Heels, Shoulders, Buttocks & Head Erect	1585
Sitting Height		Head to Seat with Body Erect	910
Neck Breadth	(y)	Lateral	110
Neck Depth	(x)	A to P	130
Upper Torso Breadth	(y)	Chest Breadth at Xiphoid	215
Shoulder Width	(y)	Biachromial Breadth	340
Lower Torso Breadth	(y)	Right to Left Iliocristale	360
Upper Leg Length	(z)	Trochanter to Femoral Condyle	345
Lower Leg Length	(z)	Tibiale to Heels	390
Head Height	(z)	Gnathion to Vertex	240
Head Breadth	(y)	Right to Left Tragion	110
Head Depth	(x)	Ophistocranon to Glabella	190
Head Circumference		Above Brow Ridge	610
Upper Torso Depth	(x)	Chest Depth at Xiphoid	330
Lower Torso Depth	(x)	At Anterior-Superior Iliac Spine	360
Chest Circumference		At Xiphoid	990
Waist Circumference		At Most Superior Point of Pelvis	860
Top of Head to C7			225
Neck Height	(z)	C1 to C7	80
Upper Torso Height	(z)	C7 to T12	255
T1 to T3	(z)	At Posterior Processes	40
T7 to T9	(z)	At Posterior Processes	35
L1 to L3	(z)	At Posterior Processes	50
Lower Torso Height	(z)	T12 to Coccyx	280
Weight		Of Whole Body	79.0 kg

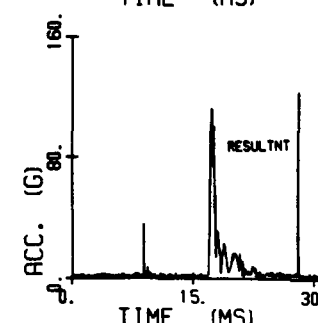
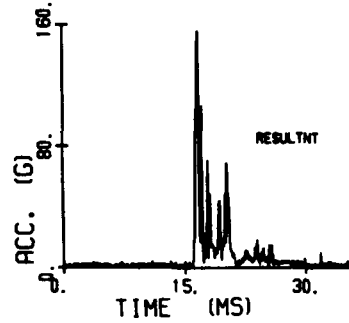
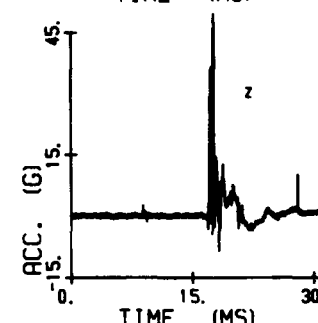
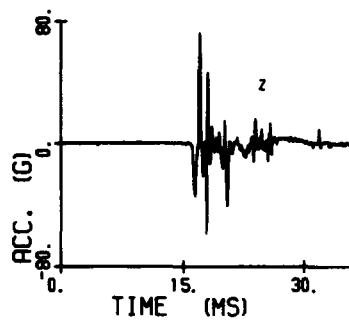
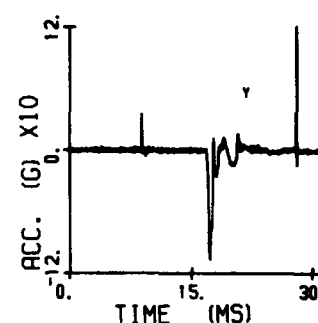
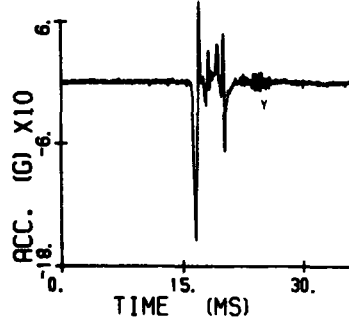
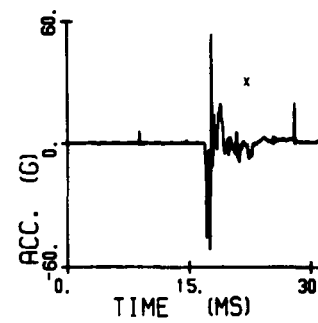
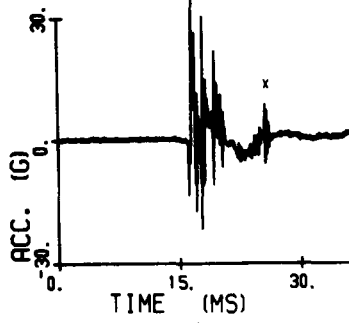
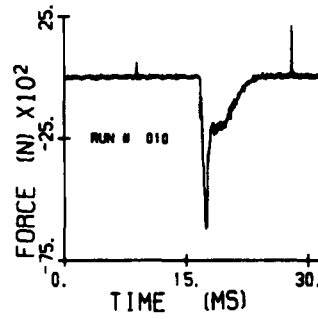
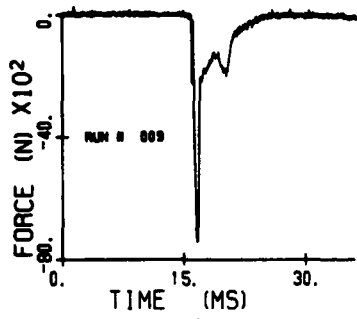
APPENDIX B
FORCE AND ACCELERATION TRACINGS FROM TEST 001-015

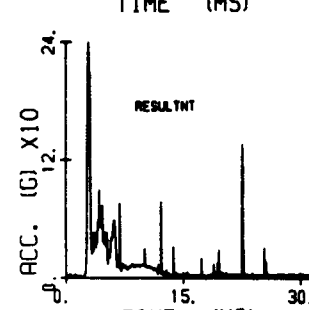
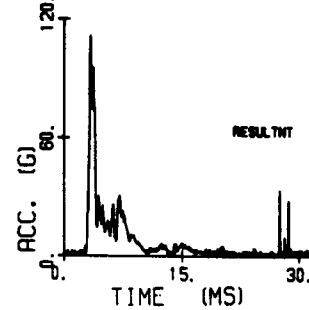
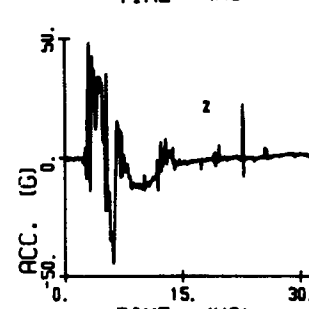
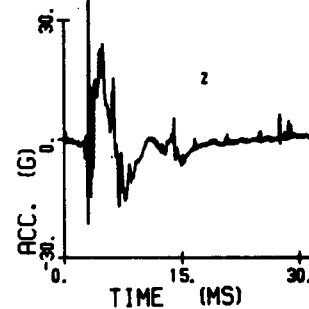
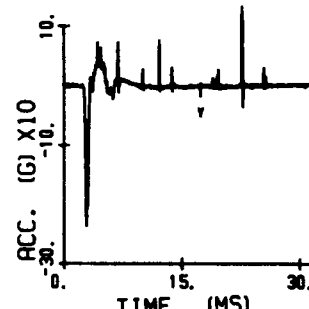
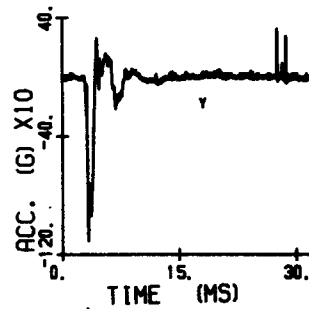
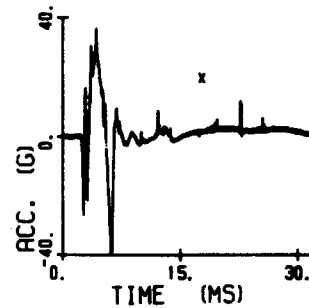
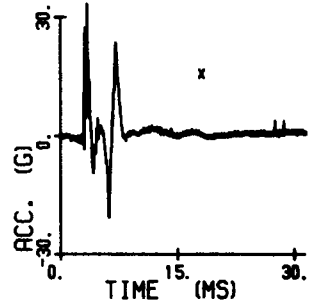
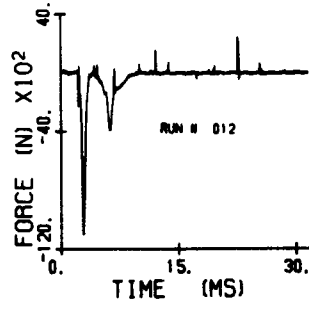
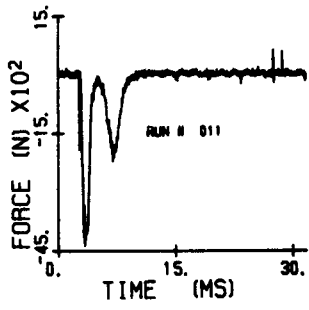


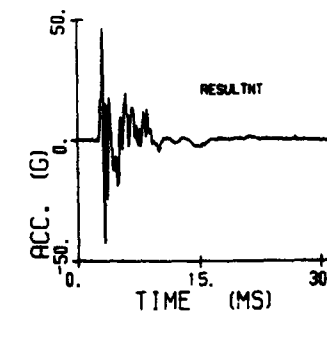
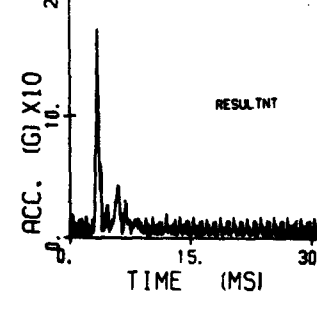
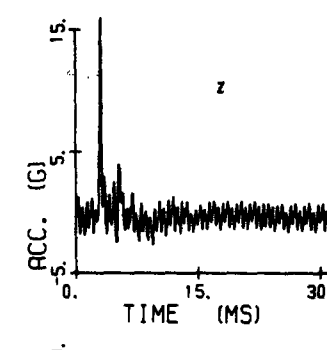
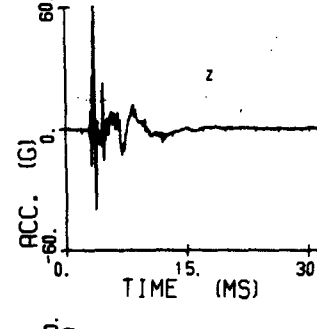
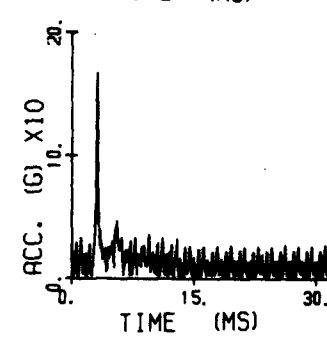
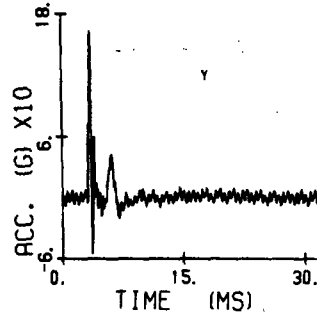
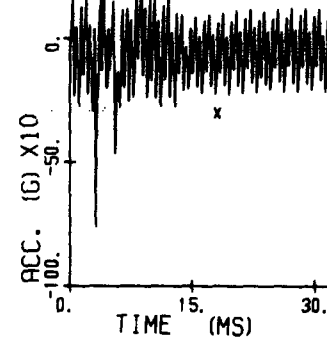
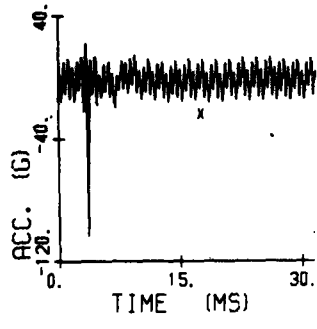
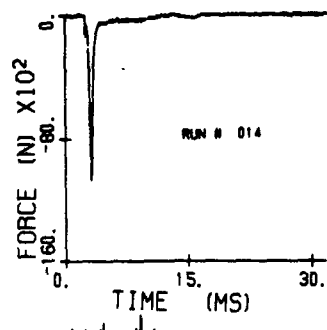
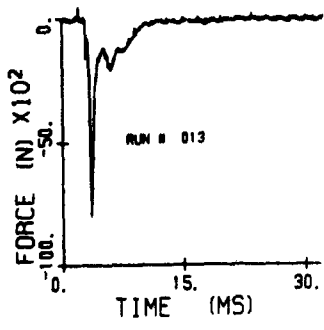


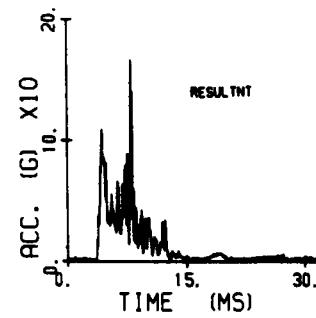
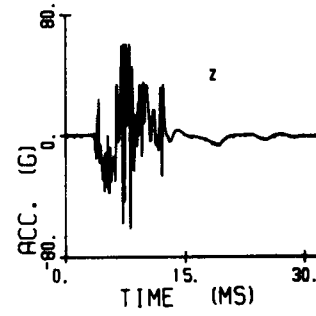
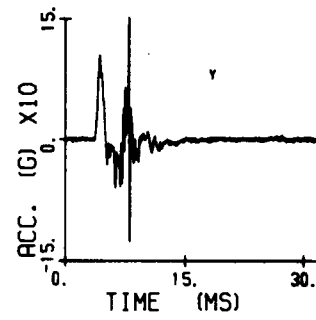
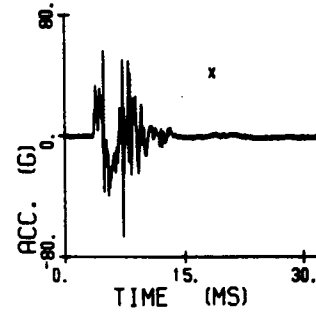
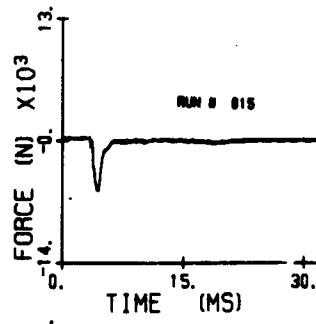












APPENDIX C
LIST OF MANUFACTURERS

Robert A. Denton, Inc.
1693 Hamlin Road
Avon Township, MI 48063

Endevco
Rancho Viejo Road
San Juan Capistrano, CA 92675